frontiers | Frontiers in Energy Research

ORIGINAL RESEARCH
published: 16 May 2022
doi: 10.3389/fenrg.2022.910304

Experimental and Numerical Studies of Ignition Delay Time and Laminar Flame Speed of JP-10at Elevated Temperature Conditions

Junsen Yang[1], Yi Wu[1], Zhenpeng Zhang[2,3], Yanlei Shang[2,3] and Lun Pan[4]*

[1]School of Aerospace Engineering, Beijing Institute of Technology, Beijing, China, [2]School of Materials Science and Engineering, Southwest Jiaotong University, Chengdu, China, [3]The Pec Institute of Multiscale Science, Chengdu, China, [4]School of Chemical Engineering and Technology, Tianjin University, Tianjin, China

In this work, the laminar flame speeds of JP-10/air mixtures and ignition delay time of JP-10/O_2/Ar mixtures have been studied over a wide range of experimental conditions using a premixed Bunsen flame and a shock tube. Laminar flame speed measurements of the JP-10/air mixture were measured at T = 360–453 K, φ = 0.7–1.3 and p = 1 atm. The ignition delay times of JP-10 with fuel mole fraction of 0.2% JP-10/2.8% O_2/97% Ar were measured with a heated shock tube behind the reflected shock wave at 1183–1478 K and pressure of 3.4 atm. Numerical calculation and sensitivity analysis of the laminar flame speed and ignition delay time of JP-10 were performed by using published detailed and skeletal kinetic mechanisms. The comparison of experimental and numerical results showed that all models tend to overestimate the laminar flame speed under the studied conditions, especially under lower temperature conditions (360–423 K). A temperature dependency empirical correlation of laminar flame speed was then proposed by power law theory. The sensitivity analysis identified three important reactions [$H+O_2$ = $O+OH$, C_5H_5+H (+M) = C_5H_6(+M), $C_3H_3+C_2H_2$ = C_5H_5] that determined the laminar flame speed and ignition delay time.

Keywords: JP-10 fuel, laminar flame speed, ignition delay time, kinetic mechanism analysis, bunsen flame

OPEN ACCESS

Edited by:
Xiao Liu,
Harbin Engineering University, China

Reviewed by:
Yiheng Tong,
China Space Foundation, China
Bo Jiang,
Nanjing University of Science and Technology, China
Yingchun Wu,
Zhejiang University, China

****Correspondence:***
Yi Wu
yi.wu@bit.edu.cn

Specialty section:
This article was submitted to Advanced Clean Fuel Technologies, a section of the journal Frontiers in Energy Research

Received: *01 April 2022*
Accepted: *19 April 2022*
Published: *16 May 2022*

Citation:
Yang J, Wu Y, Zhang Z, Shang Y and Pan L (2022) Experimental and Numerical Studies of Ignition Delay Time and Laminar Flame Speed of JP-10 at Elevated Temperature Conditions. Front. Energy Res. 10:910304. doi: 10.3389/fenrg.2022.910304

1 INTRODUCTION

JP-10 is a high volumetric energy density liquid fuel that is commonly used in ramjet, scarmjet, turbine engine and pulse detonation engines (Smith and Good, 1979; Szekely and Faeth, 1983; Antaki and Williams, 1987; Brophy and Netzer, 1999; Chung et al., 1999; Parsinejad et al., 2006; Akbar, 2012; Courty et al., 2012). Its advantages of a low freezing point, high volumetric energy density and high specific pulse make it a promising fuel candidate for applications in both civilian and military propulsion systems (Brotton et al., 2020; Wang et al., 2021). The combustion of JP-10 in a practical propulsion system is a very complex multidimensional turbulent mixing and combustion reaction process that is strongly influenced by chemical reaction kinetics (Liao et al., 2005; Gu et al., 2011; Seiser et al., 2011; Rocha, 2021; Shang et al., 2021; Wang et al., 2021; Zhang et al., 2021). Due to the different working conditions of the aircraft (such as taking off, cruising, landing, etc.), the combustion of JP-10 covers a wide range of pressure, temperature and equivalence ratio conditions (Feng et al., 2020). Therefore, it is of essential significance to accurately understand and develop chemical kinetics models valided in a wide range of conditions for the development of

TABLE 1 | Laminar flame speed studies of JP-10 in literature.

Author	Flame Configuration	T	P	Equivalence ratio range
Parsinejad et al. (2006)	Spherical flames	450–700 K	1–55 atm	0.7–1.0
Tao et al. (2018)	Counterflow flame	403 K	1 atm	0.8–1.4
	Spherical flame	600–730 K	7.5–14 atm	0.9, 1.05
Zhong et al. (2022)	Spherical flame	420 K	1 atm, 3 atm	0.7–1.3

TABLE 2 | Ignition delay time studies of JP-10 in literature.

Author	T	P	Mixture	Equivalence ratio range
Davidson et al. (2000, 2017)	950–1700 K	1–12 atm	JP-10/O_2/Ar	0.5–2.0
Colket and Spadaccini (2001)	1100–1500 K	3–8 atm	JP-10/O_2/Ar	0.5–1.5
Mikolaitis et al. (2003)	1300–2400 K	9–24 atm	JP-10/Air	1.0
Wang et al. (2007)	1000–2100 K	1.5–5.5 atm	JP-10/O_2/Ar	0.25–2.0
Xiu et al. (2018, 2020) Feng et al. (2018); Feng et al. (2020)	1400–2500 K	0.5–1 atm	JP-10/O_2/He	1

propulsion systems with high performance and high reliability (Feng et al., 2020). To develop and validate highly accurate kinetic models, it is necessary to generate experimentally obtained target parameters of the JP-10 suite for developing chemical kinetic models, such as the pyrolysis process, ignition delay time, laminar flame speed, extinction limit and soot production (Davidson et al., 2001; Nageswara Rao and Kunzru, 2006; Nakra et al., 2006; Vandewiele et al., 2014; Gao et al., 2015; Li et al., 2015; Tao et al., 2018; Johnson et al., 2020). Among these fundamental parameters, laminar flame speed and ignition delay time are the two most commonly used parameters in the evaluation of chemical kinetic models and engineering correlation (Parsinejad et al., 2006; Wang et al., 2007; Courty et al., 2012; An et al., 2015; Desantes et al., 2015).

A perfect chemical reaction kinetic model should meet the requirements of accurately predicting laminar flame speed and ignition delay time at the same time under wide range working conditions. Different from petroleum-derived fuels such as Jet A-1 and RP-3, which consist of hundreds or thousands of molecular species, JP-10 is a synthetic single-component liquid fuel (exo-tetrahydrodicyclopentadiene/exo-TCD with formula $C_{10}H_{16}$), making it a favorable target for kinetic modelling (Vandewiele et al., 2014; Zettervall, 2020). However, a summary of literature listed in **Table 1** and **Table 2** reveals that experimental measurements of laminar flame speed and ignition delay time of JP-10 have not been as extensively investigated as others, such as C_7-C_{12} hydrocarbon fuels. According to the literature, experimental measurements of the ignition delay time of JP-10 have been performed by limited studies in the last two decades (Davidson et al., 2000; Colket and Spadaccini, 2001; Mikolaitis et al., 2003; Wang et al., 2007; Gao et al., 2015).

For instance, Davidson et al. (Davidson et al., 2000) carried out a pioneering experimental measurement of the ignition delay of JP-10/O_2/Ar mixtures behind reflected shock waves with a temperature range of 1200–1700 K. Colket et al. (Colket and Spadaccini, 2001) and Mikolaitis et al. (Mikolaitis et al., 2003) also measured the ignition time of JP-10/air mixtures at almost the same period with higher temperature and pressure conditions. More recently, Gao et al. (Gao et al., 2015) revisited the ignition delay time measurements of JP-10 by using a shock tube system and proposed a new detailed kinetic model. Compared with the ignition delay time, the experimentally obtained laminar flame speed of JP-10 in the literature is even more limited. Parsinejad et al. (Parsinejad et al., 2006) measured the laminar flame speed of a JP-10/air mixture by using a constant volume chamber under various conditions. Courty et al. (Courty et al., 2012) also measured the laminar flame speed of JP-10/air mixtures at an equivalent ratio of 0.7–1.4 and a preheating temperature of 353–453 K. More recently, Zhong et al. (Zhong et al., 2022) measured the laminar flame speed of a JP-10/air mixture at a temperature of 420 K, equivalence ratio of 0.7–1.3 and pressure of 0.1–0.3 MPa. It can be seen that in addition to the limited experimental data for both ignition delay and laminar flame speed, considerable data discrepancies exist among these experiments, making it difficult to refine the developed kinetic mechanism. Therefore, new and accurate measurements are still needed for the ignition delay and linear flame speed of JP-10 in a large range of working conditions.

Apart from the fundamental experimental investigations of JP-10, such as lamianr flame speed and ignition delay time measurements, various kinetic modelling investigations of JP-10 were also conducted (Li et al., 2001; Courty et al., 2012; Gao et al., 2015; Tao et al., 2018; Zettervall, 2020; Zhong et al., 2022). According to the different application situations, the kinetic mechanism of JP-10 can be divided into two types, i.e., combustion and pyrolysis kinetic mechanism. For instance, Li et al. (Li et al., 2001) developed the first combustion kinetic mechanism of JP-10 consisting of 170 reactions and 36 species. Magoon et al. (Magoon et al., 2012) developed a detailed kinetic mechanism consisting of 320 reactions and 7740 reactions. Gao et al. (Gao et al., 2015) obtained a detailed mechanism containing 15518 reactions and 691 species by adding the oxidation reactions into the model of pyrolysis of JP-10 developed by Vandewiele et al. (Vandewiele et al., 2015). However, a detailed kinetic model cannot be efficiently used in high-dimensional CFD numerical

TABLE 3 | Combustion mechanism studies of JP-10 in literature.

Mechanism	Species numbers	Reaction numbers	Author	Experiment for validation
UCSD	36	174	Li et al. (2001)	
Magoon	320	774	Magoon et al. (2012)	
Gao	691	15518	Gao et al. (2015)	species files
Hychem detailed	120	841	Tao et al. (2018)	IDT and LFS and species files
Hychem skeletal	40	232	Tao et al. (2018)	
Z77	30	77	Zetterval (2020)	
Zhong	189	1287	Zhong et al. (2022)	LFS

simulations. More recently, skeletal kinetic models of JP-10 have been developed. For instance, Zettervall et al. (Zettervall, 2020) developed a combustion kinetic model of 30 species and 77 irreversible reactions. Zhong et al. (Zhong et al., 2022) recently proposed a new simplified JP-10 kinetic mechanism consisting of 189 species and 1287 reactions. All of these previous works have made considerable contributions to the development of accurate and useful kinetic mechanisms. Meanwhile, the discrepancy among different kinetic models remains large, and the accuracy in predicting the laminar speed and ignition delay time of laminar flame still needs further study. Reported combustion mechanisms of JP-10 are listed in **Table 3**.

It can be seen from the literature summary that the research on the combustion mechanism of JP-10 is not sufficient at present. From the development process of the mechanism, it is mainly to simplify and integrate the early mechanism and modify it in combination with the experimental data. The new mechanism developed has not been fully verified, especially in the measurement of laminar flame speed, only three published literatures reported their measurement data. The objective of the present work is to fill the measurement gap of laminar flame speed below 450 K, widen the measurement range of equivalence ratio and provide new data of ignition delay time of JP-10. To this end, the following work was carried out. First, the laminar flame speed measurements of JP-10 were performed under a wide range of temperatures and equivalence ratios of T = 360–453 K and φ = 0.7–1.3 under atmospheric pressure conditions. Second, the ignition delay time of JP-10/O_2/Ar mixture with equivalence ratio of 1.0, pressure of 3.4 atm and temperature range of 1183–1478 K was measured by a shock tube system. The experimental results of both laminar flame speeds and ignition delay times are compared with literature data. Third, numerical calculation of the laminar flame speed and ignition delay time was performed using mechanisms of JP-10 found in the literature. Finally, the chemical kinetic characteristics and structure of one-dimensional flames simulated by using different kinetic models of JP-10 are analysed and disccused in detail.

2 EXPERIMENTAL DETAILS

The samples of JP-10 fuel used in this work are provided by the research team from School of Chemical Engineering and Technology, Tianjin University (Jia, 2021; Liu et al., 2022; Qin et al., 2018; Gong et al., 2017). Since the main ingredient of JP-10 fuel, exo-tetrahydrodicyclopentadiene ($C_{10}H_{16}$), is over 96% weight fraction, it could be considered as a kind of single component fuel in research to simplify theoretical modeling. In the present work, laminar flame speed and ignition delay time measurements were performed over a wide range of conditions.

2.1 Laminar Flame Speed

Laminar flame speeds of JP-10 were measured by using a Bunsen flame burner at T = 360–453 K, φ = 0.7–1.3 and atmospheric pressure conditions. All the measurement of laminar speed in the present work is carried out with the Reynolds number of burner outlet gas flow = 1200. **Figure 1** illustrates the experimental laminar flame speed measurement system. The system consists of a Bunsen flame burner, temperature control system, gas feeding lines and optical system.

The burner consists of two contoured nozzles: the first nozzle has an outlet diameter of d_1 = 7 mm to produce the main flame (JP-10/N_2/O_2 mixture), and the second nozzle surrounds the central nozzle with an inner diameter of d_2 = 7.5 mm to obtain a pilot flame (CH_4/air mixture), which anchors the laminar premixed flame and broadens the equivalence ratio range for determination. Previous studies (Wu et al., 2016; Wu et al., 2017) have shown that the influence of pilot flame on the measurement results is negligible. To minimize the effect of the pilot flame on any possible disturbances on the main flame, the methane/air mixture flowrate for the pilot flame is kept as low as reasonably achievable. The burner is filled with ceramic beads to ensure full mixing of fuel and air and to maintain the laminar flow at the nozzle exit. Liquid fuel is stored in a stainless-steel tank and pressurized into a vaporization system (controlled evaporator and mixer/CEM-Bronkhorst) with temperature heating control. The flow rate of liquid fuel and all the gas flow are regulated by a Bronkhorst mass flow controller. Since the carrier gas in the vaporization system adds additional N_2 to the final mixture, the initial supply of N_2/O_2 should be specially adjusted to reproduce the synthetic species composition of air and modify the equivalence ratio of the fuel/air mixture. To avoid condensation of the vaporized liquid fuel and preheating the fuel/air mixture to set values, the feeding lines were wrapped with a flexible heating band, and two circulation heaters were added to the feeding lines. The flow rate and equivalence ratio are regulated and monitored by LabView code. The gas flow temperature of the nozzle outlet which is one of the experimental variables is monitored by another type K thermocouple before and after the image capturing. According to the experience in our experiment, the error range of temperature is limited in 3 K.

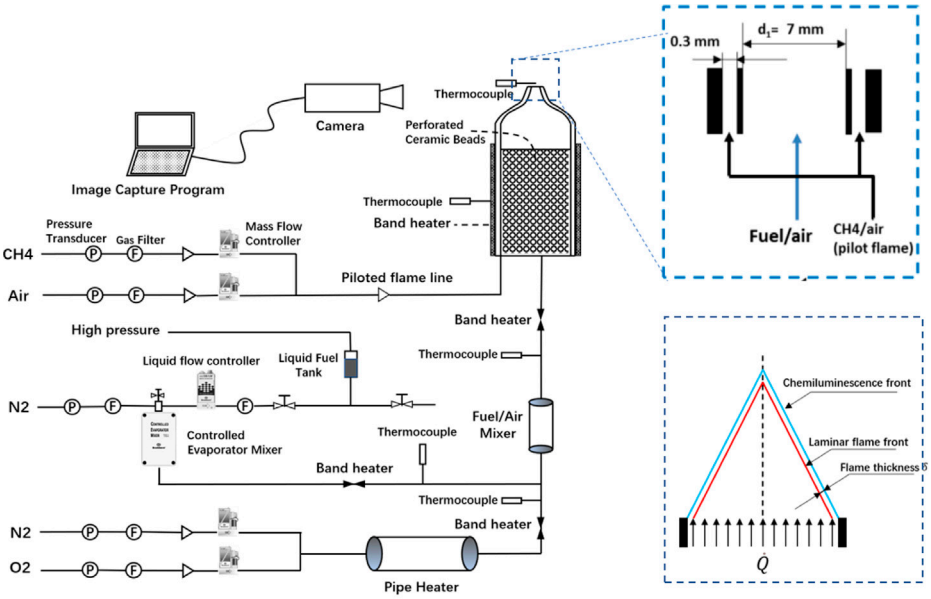

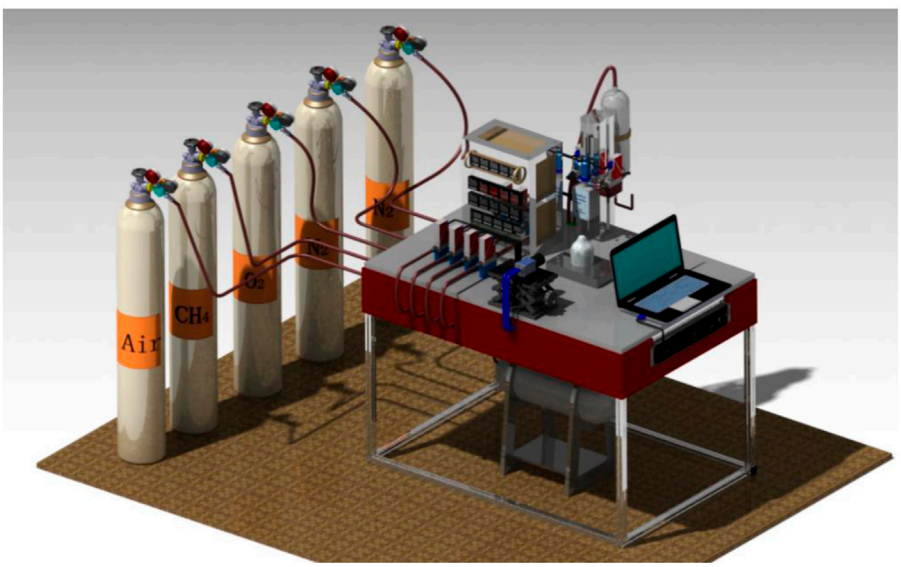

FIGURE 1 | Schematic of the experimental setup of laminar flame speed measurements.

The optical diagnostic is based on a CMOS dual-USB3 camera (Alkeria Celera C2K-M) with a 2048*1088 array. This camera is equipped with a f/16, f = 12 mm, achromatic lens. The area captured by the camera is approximately 100*100 mm^2 so that the pixel resolution of the optical system is 100 μm per pixel. The image acquisition frequency of the camera is kept at 10 Hz. The exposure time of the camera is set in 2000–3000 μs to record the flame image.

The flame area method is used here to determine the laminar flame speed S_L. Given the assumption that the laminar flame speed is the same at the entire flame front surface, the laminar flame speed can be deduced by the law of conservation of mass as follows:

$$\rho_u S_L A = \rho_u \dot{Q} \rightarrow S_L = \dot{Q}/A \tag{1}$$

where $\dot{Q}$ is the volumetric flow rate of the unburned gases at the burner outlet, ρ_u is the density of the unburned gases and A is the flame area at the appropriately chosen location.

ρ_u and $\dot{Q}$ can be calculated accurately since the mass flow rate of fuel and oxidizer gases are regulated by the liquid or gas flow controllers. The flame surface A is obtained by image processing. The recorded flame images are processed by a MATLAB program that is designed to capture the flame front profile based on the inverse Abel transformation. The flame surface area is derived by **Eq. 2**, and **Eq. 1** is used to deduce the laminar flame speed.

$$A = 2\pi \int_a^b f(x)\sqrt{1 + [f'(x)]^2}\,dx \tag{2}$$

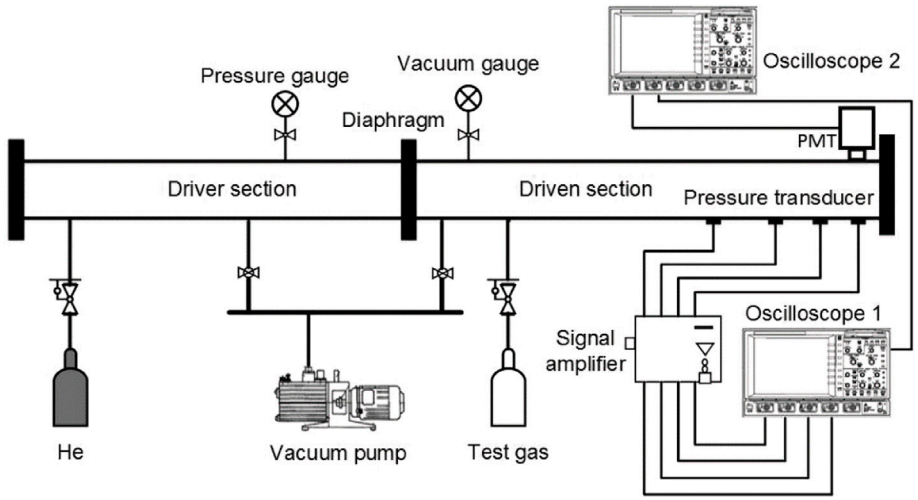

FIGURE 2 | schematic of the shock tube experiments (PMT: photomultiplier).

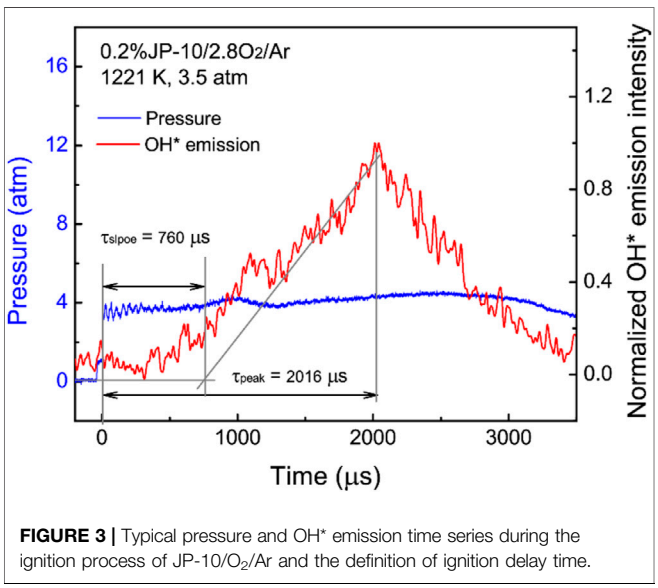

FIGURE 3 | Typical pressure and OH* emission time series during the ignition process of JP-10/O_2/Ar and the definition of ignition delay time.

where a and b are the boundary limits of integration. $f(x)$ is the flame contour profile obtained by image processing. More details on the experimental system and measurement methodology of the laminar flame speed can be found in our previous publications (Wu et al., 2016; Wu et al., 2017).

To reduce the measurement errors in the experiments and data processing, for each operating condition of all the measurements, at least 30 instantaneous images are recorded, and the averaged image is used to calculate the final flame speed. The uncertainty of the determination mainly comes from two resources: the uncertainty of the mass flow rate control (U_{Qm}) and the uncertainty of the calculation of the flame area (U_A). According to the parameters provided by Bronkhorst flow controllers, U_{Qm} is estimated to be ~2%, which roots in 0.5% of reading and 0.1% of full scale. U_A mainly comes from the pixel resolution of images recorded by the camera, which is estimated to be ~3%. The total uncertainty is equal to ~5% deduced from the equation $U = \sqrt{U_{\mathrm{Qm}}^2 + U_A^2}$.

2.2 Ignition Delay Time Measurements

The ignition delay times of JP-10 diluted in Ar are measured in a heated shock tube at Southwest Jiao Tong University, and more details of this apparatus are available in published papers (Shi et al., 2016; Shang et al., 2019). Briefly, as illustrated in **Figure 2**, this shock tube with a 50 mm inner is divided into the driver section (3.26 m) and driven section (4.52 m) by the diaphragms. The tested JP-10/O_2/Ar mixtures were preprepared in a 15 L stainless steel tank using the manometric method. To ensure the gas phase of JP-10, the driven section, mixing tank, and manifolds are heated by wrapped heating taps at 70°C. Since the main component of JP-10 is high-carbon molecule $C_{10}H_{16}$, the saturated vapor pressure at room temperature is less than 400 Pa which means the adsorption in the shock tube would be the main problem to the measurement. The purpose of dilution with Ar is to reduce the adsorption amount of JP-10 in the driven section of the shock tube as much as possible to ensure that the measured equivalence ratio is accurate. During the mixture preparation, the partial pressure of JP-10 is kept less than 0.5 kPa, which is much lower than its saturated vapor pressure at 70°C (2.48 kPa) (Cooper et al., 2002). The prepared mixtures should be allowed to diffuse completely for at least 4 h to achieve homogeneity. Before each experiment, the entire shock tube is evacuated to near vacuum by a vacuum pump.

TABLE 4 | combustion kinetic mechanism used in the present work.

	Species number	Reaction number
UCSD Li et al. (2001)	36	206
Hychem detailed Tao et al. (2018)	120	841
Hychem skeletal Tao et al. (2018)	40	232

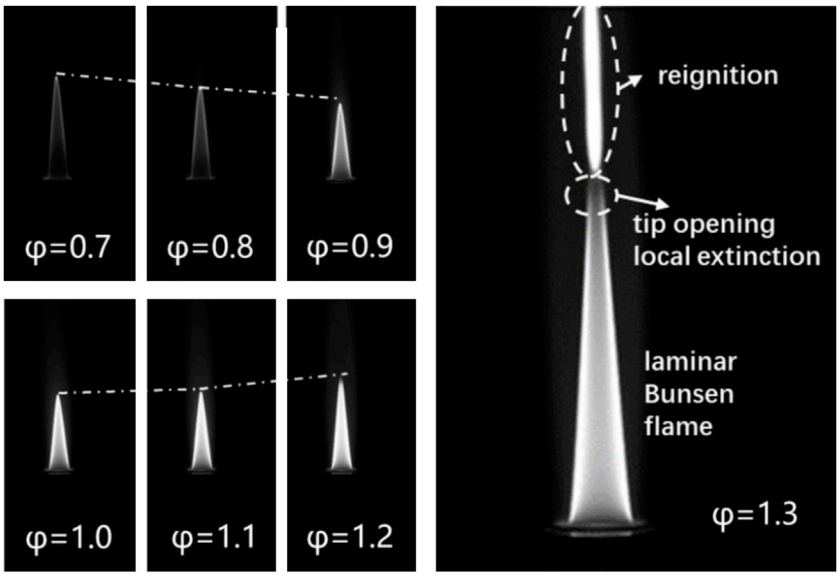

FIGURE 4 | Flame images of the JP-10/air mixture at T = 453 K and φ = 0.7–1.3.

Helium gas is used as the driver gas, and the different temperatures (T) and pressures (*p*) after the reflected shock wave are controlled by adjusting the injection pressures of the driver and driven section. The gas leakage of the system is less than 1 Pa min^{-1}.

Four pressure sensors are fixed along the driven section close to the endwall to determine the shock wave speed, and the OH* emission (307 nm) during fuel ignition is captured by a photomultiplier at the sidewall. **Figure 3** shows the typical pressure and OH* emission time series during the ignition process of JP-10 at 1221 K and 3.5 atm. Consistent with the previous literature (Mikolaitis et al., 2003), the OH* emission has a low intensity with a broad shape. The ignition delay time is defined as the time interval between the onset of the reflected shock wave and the intersection of the baseline with the maximum gradient (τ_{slope}) or the corresponding peak (τ_{peak}) of the OH* emission profile. The uncertainty of the measured ignition delay times is less than 20%.

2.3 Chemical Kinetic Modelling

Calculations are carried out to verify the experimental laminar flame speed and ignition delay time of the JP-10/air mixture. The one-dimensional premixed laminar flame is simulated by premixed laminar flame-speed calculation model, while the ignition delay time is simulated in closed homogeneous batch reactor. For laminar flame speed simulation, the mixture average transport scheme is used, the GRAD and CURV parameters are set to 0.1, and the grid number is large enough to ensure the convergence of the final solution. For ignition delay time simulation, the constant volume approach is used. In the present work, three combustion kinetic mechanisms of JP-10/air are used, i.e., the UCSD (Li et al., 2001), Hychem skeletal and detailed mechanisms developed in Tao's work (Tao et al., 2018). As illustrated in **Table 4**, the UCSD mechanism consists of 36 species and 206 reactions, the Hychem detailed mechanism uses 120 species and 841 reactions, and the Hychem skeletal mechanism reduced from the detailed one includes 40 species and 232 reactions.

TABLE 5 | Summary of the Lewis number of unburned mixtures in the present work calculated with Hychem detailed mechanism.

Temperature	Lewis number	
	φ = 0.7	φ = 1.3
360 K	2.943	0.957
423 K	2.938	0.955
453 K	2.935	0.954

3 RESULTS AND ANALYSIS

3.1 Laminar Flame Speed

3.1.1 Flame Characteristics of JP-10/Air

The laminar flame speeds of JP-10 were measured under a temperature of 360–453 K and an equivalence ratio of 0.7–1.3. **Figure 4** shows the typical Bunsen flame under a preheating temperature of 453 K and atmospheric pressure conditions with constant outlet velocity. With the piloted flame, the main flame of the JP-10/air mixtures can be stabilized over a wide equivalence ratio from φ = 0.7 to φ = 1.3. In the range of equivalence ratios of 0.7–1.0, the intensity of the flame image increases with increasing equivalence ratio, and the height of the flame decreases with increasing equivalence ratio. In the range of equivalence ratios of 1.1–1.2, the opposite trend was observed. As the fuel/air mixture flow was kept constant, according to **Eq. 1**, the trend of the height variation of the flame is opposite to the laminar flame speed variation, which is indeed observed in the present work.

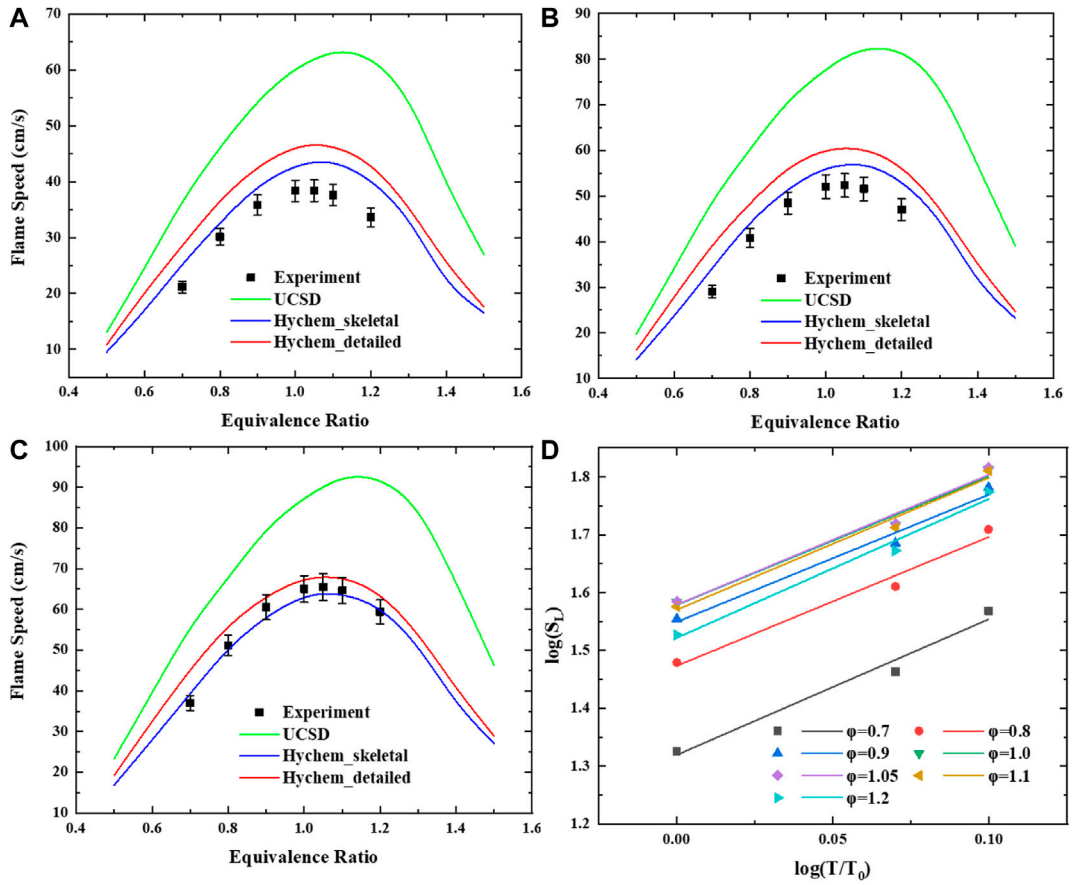

FIGURE 5 | Laminar flame speed of JP-10/air mixtures versus equivalence ratio range of 0.7–1.2 at elevated temperature: **(A)** T = 360 K. **(B)** T = 423 K. **(C)** T = 453 K. **(D)** Log-log plot of the laminar flame speed of JP-10/air under atmospheric temperature and different preheating temperatures.

TABLE 6 | parameters of $S_{L0,i}$ and α_i of correlation equations.

Reference S_{L0} parameters		Slope of Log (S_L)-log (T/T_0)		Temperature exponent $\alpha(\varphi)$ parameters	
$S_{L0,\varphi=1}$	38.79	$\alpha_{\varphi=0.7}$	2.347	α_0	2.220
$S_{L0,1}$	24.60	$\alpha_{\varphi=0.8}$	2.230	α_1	0.475
$S_{L0,2}$	−187.03	$\alpha_{\varphi=0.9}$	2.204	α_2	2.496
$S_{L0,3}$	−393.71	$\alpha_{\varphi=1.0}$	2.224	α_3	−1.597
$S_{L0,4}$	−377.90	$\alpha_{\varphi=1.05}$	2.248		
		$\alpha_{\varphi=1.1}$	2.284		
		$\alpha_{\varphi=1.2}$	2.404		

The flame tip opening phenomenon was observed when the equivalence ratio values were higher than 1.3. Under these conditions, the flame was locally quenched at the flame tip and then reignited above the tip opening region, resulting in another laminar flame with a high soot concentration. **Figure 4** shows the phenomenon of flame tip opening and reignition of the flame. It is found that for all the experimental conditions carried out in this work, no matter what temperature and outlet velocity vary, the flame tip opening phenomenon and reignition always occur once the equivalence ratio is higher than 1.3.

Some researchers have studied the flame tip opening phenomenon and attributed it to the curvature effect on nonequi-diffusive preheated mixtures of fuel/air leading to a change in the burning intensity at the flame tip (Ishizuka, 1982; Law et al., 1982; Mizomoto et al., 1985; Mizomoto and Yoshida, 1987; Sakai et al., 1996; Bouvet et al., 2011). The Lewis number, which is defined as the ratio of the mixture thermal diffusivity to the mass diffusivity of the deficient reactant, is generally considered an important parameter relevant to the flame tip opening phenomenon (Mizomoto and Yoshida, 1987). When the Lewis number of the unburned mixtures is

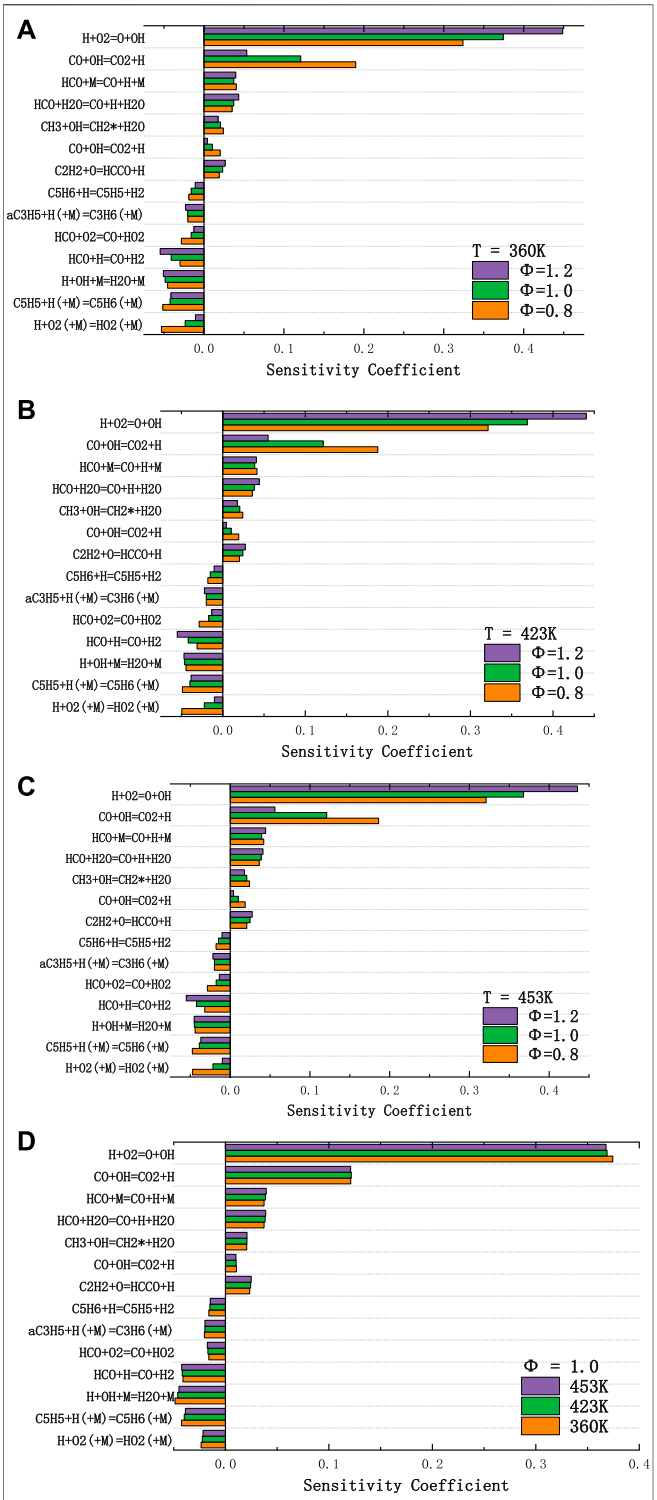

FIGURE 6 | Normalized sensitivity coefficients in predicting laminar flame speed of JP-10/air flame for T= **(A)** 360 K, **(B)** 423 K, **(C)** 453 K, and **(D)** ϕ = 1.0, caculated with Hychem detailed mechanism.

less than 1, the flame burning intensity decreases at the tip, causing local quenching of the flame. The reignited flame above the main flame could possibly be due to the fuel unburned at the tip of the flame being reignited by radiation effects. Previous investigations have found that the flame tip opening phenomenon may appear on the very lean fuel side and the very rich fuel side (Mizomoto et al., 1985; Mizomoto and Yoshida, 1987). The Lewis number of the unburned mixtures in the present work with equivalence ratio and temperature variations were calculated referring to the method of literature (Mizomoto and Yoshida, 1987). As illustrated in **Table 5**, it is observed that the Lewis number decreases with increasing temperature and decreases with increasing equivalence ratio. All the flame tip opening phenomenon observed in this work occur with a Lewis number less than 1.

3.1.2 Effect of Temperature

To investigate the sensitivity to the preheating temperature of the JP-10/air mixture, comparisons of measured and simulated laminar flame speeds for atmospheric pressure and for various preheating temperatures T = 360 K, 423 K, 453 K and φ = 0.7–1.2 are presented in **Figure 5**.

This shows that the laminar flame speed increases with increasing preheating temperature. The results calculated by using UCSD are generally higher than those calculated by the other two mechanisms and the measurements. The detailed mechanism of Hychem predicts a higher laminar flame speed than the skeletal mechanism. For low-temperature cases (T = 360 K, 423 K), the simulation using Hychem-skeletal and Hychem-detailed mechanisms overestimates the laminar flame speed compared with measurements. For higher preheating temperatures, the simulation produces a fairly close approximation of the measurements. In terms of discrepancy, the measurement results of this study are in good agreement with Hychem detailed mechanism and skeletal mechanism, and there is a large discrepancy compared with the predicted value of UCSD mechanism. Compared with the predicted value of UCSD mechanism, the absolute discrepancy is 10–20 cm/s and the relative discrepancy is 20–30%. In some data points with high equivalence ratio, the relative error is more than 30%. Other literatures also reported the great inconsistency with UCSD mechanism which may result from the overestimation of the sensitivity of cyclopentene oxidation reaction to flame speed (Zhong et al., 2022). Compared with Hychem skeletal mechanism, the absolute discrepancy is within 5 cm/s and the relative discrepancy is within 15%. The discrepancy between the experimental data and the predicted value of the mechanism at 360 K is relatively large. The measurement results reach a good consistency with predicted results at 453 K, the absolute discrepancy is within 2 cm/s and the relative discrepancy is within 5%. Compared with Hychem detailed mechanism, the absolute discrepancy is within 8 cm/s and the relative discrepancy is within 15%. The points with large discrepancy are mainly concentrated in the measurement conditions with equivalence ratio of 0.7 and 1.2. The predicted value of detailed mechanism is in good agreement with the measured value at 453 K. The absolute discrepancy of most of the points is within 3 cm/s and the relative discrepancy is within 5%.

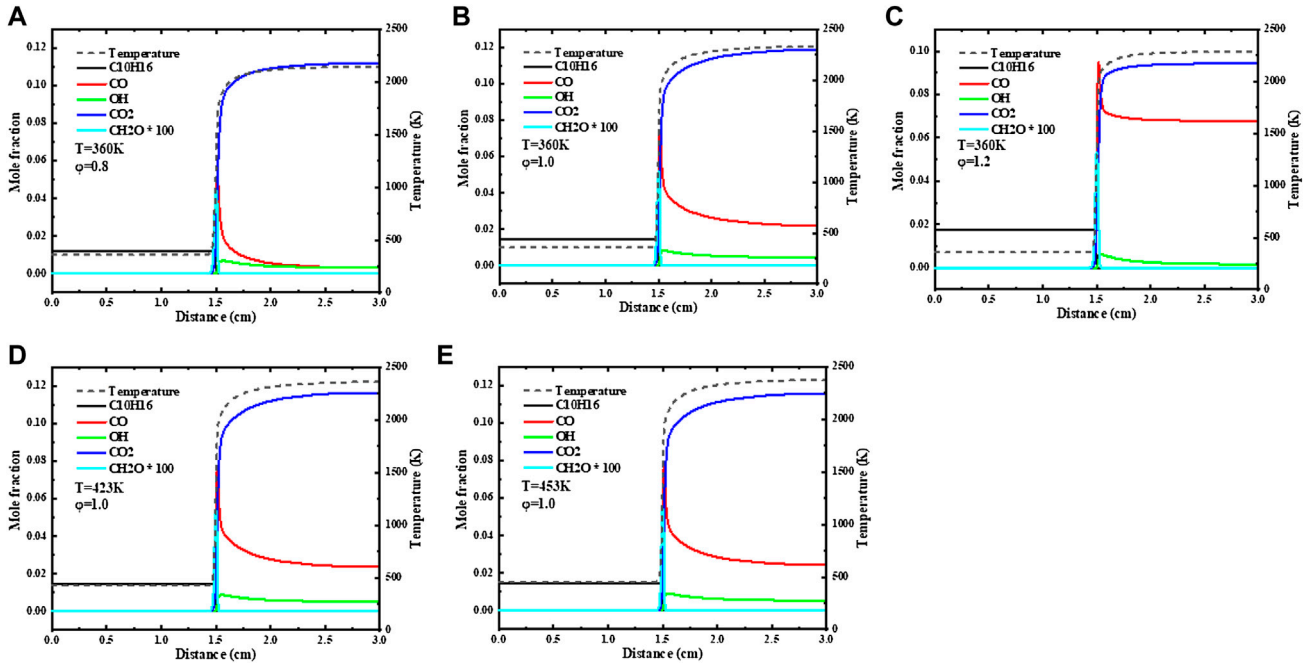

FIGURE 7 | Major species mole fraction and adiabatic flame temperature of JP-10/air flame of T = 360 K, **(A)** φ = 0.8, **(B)** 1.0, **(C)** 1.2; and φ = 1.0, T=**(D)** 423 K, **(E)** 453 K calculated with Hychem detailed mechanism.

According to the power law correlation theory of temperature dependency (Metghalchi and Keck, 1982; Varea et al., 2013) $S_L = S_{L0}(\frac{T}{T_0})^{\alpha}$, the laminar flame speed under higher temperatures can be expressed by a laminar flame speed at the reference conditions of temperature and pressure (S_{L0}) and multiplied by correction factors displaying the temperature dependencies. As shown in **Figure 5**. (d), the laminar flame speed is plotted as a function of the preheating temperature using log-log scales, while straight lines for all of the equivalence ratios tested are observed which illustrates the temperature dependence on the laminar flame speed. The power exponent $\alpha(\varphi)$ is determined from the slope of the straight lines in **Figure 5**. (d). By fitting the slope of the Log(S_L)-Log (T/T_0) lines with the third-order polynomial expression **Eq. 5**, the equivalence ratio dependence coefficients are calculated and listed in **Table 6**.

With the experimental results obtained in the present work, an empirical temperature dependency correlation was proposed by using the power law equation **Eqs. 3–5**, where S_{L0} is the flame speed at T = 360 K, p = 0.1 MPa.

$$S_L = S_{L0}\left(\frac{T}{T_0}\right)^{\alpha} \tag{3}$$

$$S_{L0}(\varphi) = S_{L0,\varphi=1} + S_{L0,1}(\varphi-1) + S_{L0,2}(\varphi-1)^2 + S_{L0,3}(\varphi-1)^3 + S_{L0,4}(\varphi-1)^4 \tag{4}$$

$$\alpha(\varphi) = \alpha_0 + \alpha_1(\varphi-1) + \alpha_2(\varphi-1)^2 + \alpha_3(\varphi-1)^3 \tag{5}$$

3.1.3 Kinetic Analyses

Sensitivity analysis is conducted to identify the important reactions related to JP-10/air laminar flame speed, and fourteen reactions with the largest magnitude of sensitivity coefficient are presented in **Figure 6**. The Hychem detailed mechanism is chosen in the premixed flame simulation for ϕ = 0.8, 1.0, and 1.2 at 1 atm and T = 360 K, 423 K, and 453 K. The normalized sensitivity coefficient (S_i) of the laminar flame speed is calculated using the following formula:

$$S_i = \frac{A_i}{S_L}\frac{\partial S_L}{\partial A_i} \tag{6}$$

where A_i is the pre-exponential factor of the ith reaction. The positive sensitivity indicates that the reactions increase the flame speed, and the negative sensitivity indicates that the reactions slow down the flame speed.

The sensitivity coefficient of most reactions decreases with increasing reaction temperature. Fourteen reactions with the largest magnitude of sensitivity coefficient show that the chain branching reaction H+O_2 = O+OH and chain propagation reaction CO+OH = CO_2+H dominate the chemistry of flame propagation under all conditions studied in the present work. On the other hand, the chain termination reactions H+OH+M = H_2O+M, H+O_2 (+M) = HO_2(+M) and C_5H_5+H (+M) = C_5H_6(+M) play an important role in the slowing the flame speed. The H+O_2 = O+OH reaction is the most sensitive reaction to the flame propagation speed. The formation of the reaction product OH largely affects another reaction with a large sensitivity coefficient, CO+OH = CO_2+H, which in turn affects the rate at which fuel oxidizes to the final product CO_2. At the same time, the competitive reaction of H+O_2 = O+OH, H+O_2 (+M) = HO_2(+M) slows the production of OH, and the

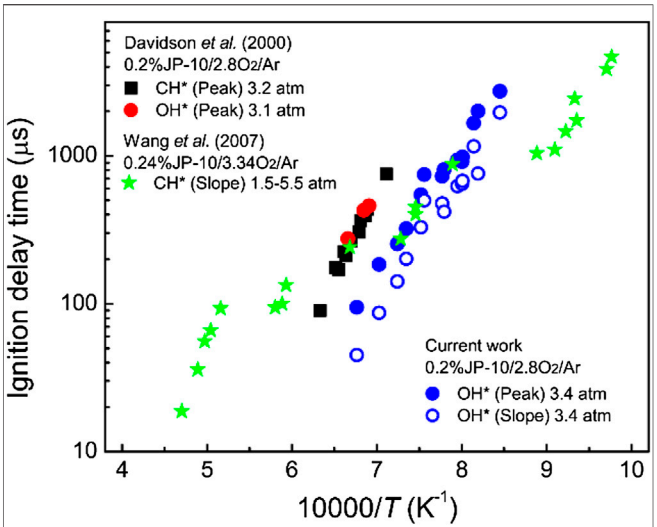

FIGURE 8 | Comparison between our measured ignition delay times and the reported values from the literature (Davidson et al., 2000; Wang et al., 2007).

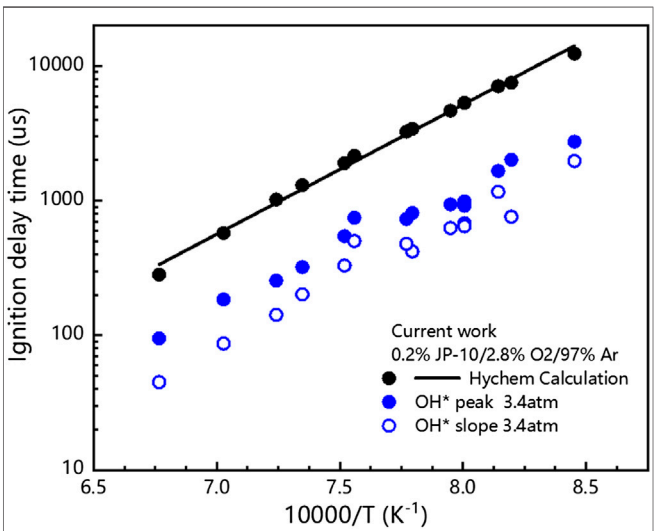

FIGURE 9 | Comparison between our measured ignition delay times and the calculated values with Hychem detailed mechanism.

competitive reaction of CO+OH = CO_2+H, H+OH+M = H_2O + M hinders the oxidation of CO, so these two reactions with large negative sensitivity coefficients reduce the flame propagation speed. In addition, the reactions C_5H_6+H=C_5H_5+H_2, C_5H_5+H (+M) = C_5H_6(+M) and C_5H_6+H=C_5H_5+H_2 related to the pyrolysis products of JP-10 promote and retard the flame propagation speed, respectively.

Figure 7 gives the simulation results of the 1-D flame structure. The adiabatic flame temperature and the mole fraction of some major species related to flame propagation chemistry show the flame structure of JP-10 at initial temperatures of 360 K, 423 K, and 453 K and a pressure of 1 atm. Under the lean fuel condition of equivalence ratio φ = 0.8, the mole fraction of CO is significantly lower than that under stoichiometric ratio conditions and under rich-fuel conditions, and the mole fraction difference at chemical equilibrium between CO_2 and CO reaches a level close to 0.1, which indicates that CO has been fully oxidized and to a certain extent also illustrates the full combustion of JP-10 fuel.

As the equivalence ratio increases, the mole fraction difference at chemical equilibrium between CO_2 and CO continues to shrink. Under the condition of equivalence ratio φ = 1.2, the peak concentration of CO is even higher than the peak concentration of CO_2, which indicates that CO has not been fully oxidized. The change of CH_2O mole fraction with temperature is not significant, but the change trend with equivalence ratio is the same as that of flame speed, which first increases and then decreases. From the previous laminar flame speed sensitivity analysis, it can be seen that H+O_2 = O+OH and CO+OH = CO_2+H are the two most sensitive reactions regarding the laminar flame speed. Therefore, under rich fuel conditions, the relative shortage of O_2 and the relative excess of CO may lead to a decrease in reactivity, which may be one of the reasons for the decrease in laminar flame speed. The flame combustion temperature increases with increasing equivalence ratio, but in the process of increasing the equivalence ratio from 1 to 1.2, the change in the adiabatic flame temperature is not obvious, which also reflects the temperature dependence of the laminar flame speed. Within the range of equivalence ratios φ = 0.7–1.2, the increase in laminar flame speed is more obvious than that in the range of 1–1.2.

3.2 Ignition Delay Time

3.2.1 Comparison of Experimental Results

The measured ignition delay times of JP-10/O_2/Ar mixtures are shown in **Figure 8**, and the available values from the literature (Davidson et al., 2000; Wang et al., 2007) are also adopted for comparison. The ignition delay time of JP-10 decreases markedly with increasing temperature, and the τ peak decreases from 2016 μs at 1221 K to 185 μs at 1422 K. Our measurements have a similar temperature dependence but give lower values in comparison to those of Davidson et al. (Davidson et al., 2000). At temperatures of 1249–1381 K, our measured ignition delay times agree well with the results of Wang et al. (Wang et al., 2007). In the investigated temperature range, however, the reported ignition delay times of JP-10 do not match well with each other. Due to the varying industrial standards, production processes, and preservation conditions, the constituents of JP-10 are usually slightly different. To confirm the reliability of the ignition delay times, some points are repeatedly measured at least two times, and the results indicate that our measurements are credible.

3.2.2 Sensitivity Analysis of Ignition Delay Time

In this work, the detailed mechanism of the hychem is selected to simulate the ignition process of JP-10. The reaction model is a closed homogeneous batch reactor. In the simulation calculation, the time corresponding to the intersection of the tangent at the

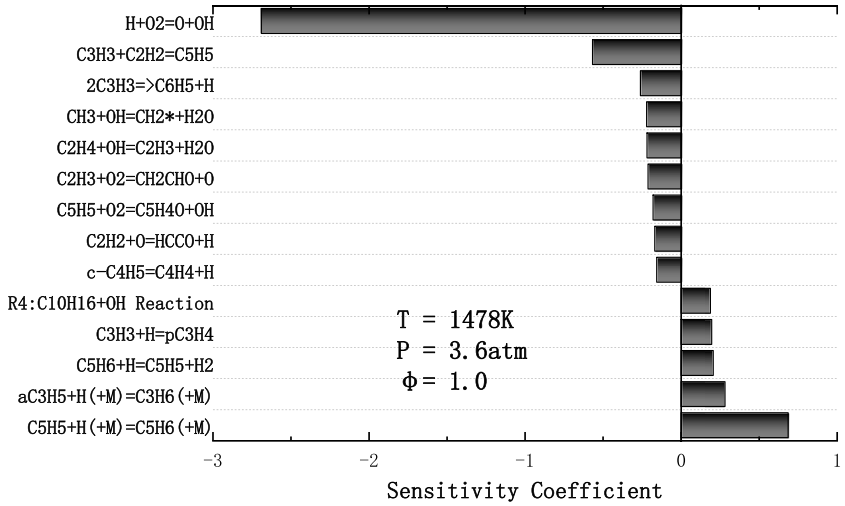

FIGURE 10 | Normalized sensitivity coefficients in predicting ignition delay time of JP-10/O_2/Ar mixture for T = 1478 K, p = 3.6 atm, φ = 1.0 calculated with Hychem detailed mechanism.

maximum slope of the temperature curve and baseline is defined as the ignition time.

Figure 9 shows the measurement results of the ignition delay time of JP-10 and the numerical calculation results using the detailed mechanism of Hychem. **Figure 9** shows that the ignition delay time decreases with increasing premixed gas temperature, and the premixed gas needs a longer time to absorb heat at lower temperatures to reach the ignition conditions. As mentioned above, the experimental data obtained in this paper show an overall smaller trend compared with the experimental data under similar working conditions in the literature, and it is also lower compared with the numerical calculation results, which may be related to the differences in the definitions of ignition delay time and experimental samples.

To further explore the key reactions leading to the ignition process, sensitivity analysis was carried out on the basis of the Hychem mechanism. The sensitivity coefficient is defined as

$$S = \frac{\tau(2.0k_i) - \tau(0.5k_i)}{1.5\tau(k_i)} \tag{7}$$

where τ is the ignition delay time and k_i is the pre-exponential factor of the ith reaction. In this paper, the positive sensitivity coefficient indicates that it can inhibit the ignition process, and the negative sensitivity coefficient indicates that it can promote the ignition process. **Figure 10** shows the key sensitive reactions of JP-10/O_2/Ar mixture ignition at T = 1478 K, p = 3.6 atm and φ = 1.0.

As shown in **Figure 10**, the chain branching reaction $H+O_2 = O+OH$ dominates the ignition chemical process of JP-10. One of the fourteen most important reactions is related to JP-10 fuel. R4 involves the cracking of fuel into C_2, C_3, and C_5 low-carbon molecules, while other key reactions are related to these low-carbon molecules. The reaction of C_3H_3 and C_2H_2 to produce C_5H_5 has a significant impact on the ignition process, and the second largest negative sensitivity coefficient is given. Small radical reactions such as OH have a significant impact on the ignition delay time and participate in most of the fourteen key radical reactions. In addition, the bonding reaction of C_3H_5 and C_5H_5 absorbing H radicals can inhibit the ignition process.

4 CONCLUSION

As a high-density hydrocarbon fuel, JP-10 has an excellent application prospect in the field of aircraft propulsion system, but there are few studies on its combustion kinetics and experimental measurement to verify these mechanisms. In this paper, the basic combustion characteristics of JP-10 (laminar flame speed, ignition delay time) are measured, and kinetic studies are conducted to verify the reported mechanism. The main conclusions are as follows:

1) Experimental study on laminar flame speed of JP-10/air mixture were conducted in Bunsen burner at different equivalence ratios (0.7–1.2), temperatures (360–453 K), atmosphere pressure. Correlation of laminar flame speed is given according to the power law correlation theory of temperature dependency. The comparison between experimental data and mechanism prediction shows that the UCSD mechanism has an overestimation trend in predicting laminar flame speed and the prediction of Hychem mechanisms (detailed and skeletal) is in good agreement with experimental data.
2) Experimental study on ignition delay time of 0.2%JP-10/2.8% O_2/97%Ar mixture were conducted in shock tube at different temperatures (1183K–1478K), 3.4 atm. The comparison shows that the Hychem detailed mechanism overestimates the ignition delay time at our experimental conditions.

3) Kinetic studies show that there are three reactions ($H+O_2$ = O+OH, C_5H_5+H (+M) = C_5H_6(+M), $C_3H_3+C_2H_2$ = C_5H_5) determine the laminar flame speed and ignition delay time at tested temperature and equivalence ratio range.

DATA AVAILABILITY STATEMENT

The original contributions presented in the study are included in the article/**Supplementary Material**, further inquiries can be directed to the corresponding author.

AUTHOR CONTRIBUTIONS

JY (First author): experiment, data processing, writing original draft, conceptualization, methodology; YW (corresponding author): funding acquisition, data curation, writing original draft, supervision; ZZ: experiment, writing original draft, review and; editing; YS: data processing, writing original draft; LP: providing JP-10 fuel, review and; editing.

FUNDING

This research is supported by National Natural Science Foundation of China No.51906016.

SUPPLEMENTARY MATERIAL

The Supplementary Material for this article can be found online at: https://www.frontiersin.org/articles/10.3389/fenrg.2022.910304/full#supplementary-material

Supplementary Table S1 | Measured ignition delay times of JP-10/O2/Ar.

Supplementary Table S2 | Measured laminar flame speed (cm/s) of JP-10/air.

REFERENCES

Akbar, R. (2012). "Detonation Properties of Unsensitized and Sensitized JP-10 and Jet-A Fuels in Air for Pulse Detonation Engines," in 36th AIAA/ASME/SAE/ASEE Joint Propulsion Conference and Exhibit., Las Vegas, NV, July 24–28, 2000.

An, Y.-z., Pei, Y.-q., Qin, J., Zhao, H., and Li, X. (2015). Kinetic Modeling of Polycyclic Aromatic Hydrocarbons Formation Process for Gasoline Surrogate Fuels. *Energy Convers. Manag.* 100, 249–261. doi:10.1016/j.enconman.2015.05.013

Antaki, P., and Williams, F. A. (1987). Observations on the Combustion of Boron Slurry Droplets in Air. *Combust. Flame* 67 (1), 1–8. doi:10.1016/0010-2180(87)90009-5

Bouvet, N., Chauveau, C., Gökalp, I., Lee, S.-Y., and Santoro, R. J. (2011). Characterization of Syngas Laminar Flames Using the Bunsen Burner Configuration. *Int. J. Hydrogen Energy* 36 (1), 992–1005. doi:10.1016/j.ijhydene.2010.08.147

Brotton, S. J., Malek, M. J., Anderson, S. L., and Kaiser, R. I. (2020). Effects of Acetonitrile-Assisted Ball-Milled Aluminum Nanoparticles on the Ignition of Acoustically Levitated Exo-Tetrahydrodicyclopentadiene (JP-10) Droplets. *Chem. Phys. Lett.* 754, 137679. doi:10.1016/j.cplett.2020.137679

Brophy, C., and Netzer, D., (1999). "Effects of Ignition Characteristics and Geometry on the Performance of a JP-10/O2 Fueled Pulse Detonation Engine," in 35th Joint Propulsion Conference and Exhibit, Los Angeles, CA, June 20–24, 1999, 2635. doi:10.2514/6.1999-2635

Chung, H. S., Chen, C. S. H., Kremer, R. A., Boulton, J. R., and Burdette, G. W. (1999). Recent Developments in High-Energy Density Liquid Hydrocarbon Fuels. *Energy fuels.* 13 (3), 641–649. doi:10.1021/ef980195k

Colket, M. B., and Spadaccini, L. J. (2001). Scramjet Fuels Autoignition Study. *J. Propuls. Power* 17 (2), 315–323. doi:10.2514/2.5744

Cooper, M. A., Shepherd, J. E., Sobota, T. H., and Moore, K. C. (2002). *Thermal and Catalytic Cracking of JP-10 for Pulse Detonation Engine Applications*. Pasadena, CA: California Institute of Technology.

Courty, L., Chetehouna, K., Halter, F., Foucher, F., Garo, J. P., and Mounaïm-Rousselle, C. (2012). Experimental Determination of Emission and Laminar Burning Speeds of α-pinene. *Combust. Flame* 159 (4), 1385–1392. doi:10.1016/j.combustflame.2011.11.003

Davidson, D. F., Horning, D. C., Herbon, J. T., and Hanson, R. K. (2000). Shock Tube Measurements of JP-10 Ignition. *Proc. Combust. Inst.* 28 (2), 1687–1692. doi:10.1016/s0082-0784(00)80568-8

Davidson, D., Horning, D., Oehlschlaeger, M., and Hanson, R., (2001). "The Decomposition Products of JP-10," in 37th Joint Propulsion Conference and Exhibit, Salt Lake City, UT, July 8–11, 2001, 3707. doi:10.2514/6.2001-3707

Desantes, J. M., López, J. J., Molina, S., and López-Pintor, D. (2015). Design of Synthetic EGR and Simulation Study of the Effect of Simplified Formulations on the Ignition Delay of Isooctane and N-Heptane. *Energy Convers. Manag.* 96, 521–531. doi:10.1016/j.enconman.2015.03.003

Davidson, D. F., Shao, J., Parise, T., and Hanson, R. K. (2017). "Shock Tube Measurements of Jet and Rocket Fuel Ignition Delay Times," in presented at the 55th AIAA Aerospace Sciences Meeting, Grapevine, TX, January 9–13, 2017.

Feng, X.-t.-f. E., Pan, L., Zhang, X., and Zou, J.-J. (2020). Influence of Quadricyclane Additive on Ignition and Combustion Properties of High-Density JP-10 Fuel. *Fuel* 276, 118047. doi:10.1016/j.fuel.2020.118047

Feng, X.-t.-f. E., Zhi, X., Zhang, X., Wang, L., Xu, S., and Zou, J.-J. (2018). Ignition and Combustion Performances of High-Energy-Density Jet Fuels Catalyzed by Pt and Pd Nanoparticles. *Energy & Fuels* 32 (2), 2163. doi:10.1021/acs.energyfuels.7b03342

Gao, C. W., Vandeputte, A. G., Yee, N. W., Green, W. H., Bonomi, R. E., Magoon, G. R., et al. (2015). JP-10 Combustion Studied with Shock Tube Experiments and Modeled with Automatic Reaction Mechanism Generation. *Combust. Flame* 162 (8), 3115–3129. doi:10.1016/j.combustflame.2015.02.010

Gong, S., Zhang, X., Bi, Q., Liu, Z., and Liu, G. (2017). Experimental Measurement of JP-10 Viscosity at 242.7-753.3 K Under Pressures up to 6.00 MPa. *J. Chem. Eng. Data* 62 (11), 3671–3678. doi:10.1021/acs.jced.7b00396

Gu, X., Li, Q., Huang, Z., and Zhang, N. (2011). Measurement of Laminar Flame Speeds and Flame Stability Analysis of Tert-Butanol-Air Mixtures at Elevated Pressures. *Energy Convers. Manag.* 52 (10), 3137–3146. doi:10.1016/j.enconman.2011.05.002

Ishizuka, S. (1982). An Experimental Study on the Opening of Laminar Diffusion Flame Tips. *Symposium Int. Combust.* 19 (1), 319–326. doi:10.1016/s0082-0784(82)80203-8

Jia, T. (2021). Mechanistic Insights into the Thermal Oxidative Deposition of C10 Hydrocarbon Fuels. *Fuel* 285, 119136. doi:10.1016/j.fuel.2020.119136

Johnson, S. E., Davidson, D. F., and Hanson, R. K. (2020). Shock Tube/laser Absorption Measurements of the Pyrolysis of JP-10 Fuel. *Combust. Flame* 216, 161–173. doi:10.1016/j.combustflame.2019.11.026

Law, C. K., Ishizuka, S., and Cho, P. (1982). On the Opening of Premixed Bunsen Flame Tips. *Combust. Sci. Technol.* 28 (3-4), 89–96. doi:10.1080/00102208208952545

Li, H., Liu, G., Jiang, R., Wang, L., and Zhang, X. (2015). Experimental and Kinetic Modeling Study of Exo-TCD Pyrolysis under Low Pressure. *Combust. Flame* 162 (5), 2177–2190. doi:10.1016/j.combustflame.2015.01.015

Li, S. C., Varatharajan, B., and Williams, F. A. (2001). Chemistry of JP-10 Ignition. *AIAA J.* 39 (12), 2351–2356. doi:10.2514/2.1241

Liao, S. Y., Jiang, D. M., Cheng, Q., Gao, J., Huang, Z. H., and Hu, Y. (2005). Correlations for Laminar Burning Velocities of Liquefied Petroleum Gas-Air Mixtures. *Energy Convers. Manag.* 46 (20), 3175–3184. doi:10.1016/j.enconman.2005.03.020

Liu, Y., Shi, C., Pan, L., Zhang, X., and Zou, J.-J. (2022). Synthesis and Performance of Cyclopropanated Pinanes with High Density and High Specific Impulse. *Fuel* 307, 1219062022.

Magoon, G. R., Aguilera-Iparraguirre, J., Green, W. H., Lutz, J. J., Piecuch, P., Wong, H.-W., et al. (2012). Detailed Chemical Kinetic Modeling of JP-10 (Exo-tetrahydrodicyclopentadiene) High-Temperature Oxidation: Exploring the Role of Biradical Species in Initial Decomposition Steps. *Int. J. Chem. Kinet.* 44 (3), 179–193. doi:10.1002/kin.20702

Metghalchi, M., and Keck, J. C. (1982). Burning Velocities of Mixtures of Air with Methanol, Isooctane, and Indolene at High Pressure and Temperature. *Combust. Flame* 48, 191–210. doi:10.1016/0010-2180(82)90127-4

Mikolaitis, D. W., Segal, C., and Chandy, A. (2003). Ignition Delay for Jet Propellant 10/Air and Jet Propellant 10/High-Energy Density Fuel/Air Mixtures. *J. Propuls. Power* 19 (4), 601–606. doi:10.2514/2.6147

Mizomoto, M., Asaka, Y., Ikai, S., and Law, C. K. (1985). Effects of Preferential Diffusion on the Burning Intensity of Curved Flames. *Symposium Int. Combust.* 20 (1), 1933–1939. doi:10.1016/s0082-0784(85)80692-5

Mizomoto, M., and Yoshida, H. (1987). Effects of Lewis Number on the Burning Intensity of Bunsen Flames. *Combust. Flame* 70 (1), 47–60. doi:10.1016/0010-2180(87)90158-1

Nageswara Rao, P., and Kunzru, D. (2006). Thermal Cracking of JP-10: Kinetics and Product Distribution. *J. Anal. Appl. Pyrolysis* 76 (1), 154–160. doi:10.1016/j.jaap.2005.10.003

Nakra, S., Green, R. J., and Anderson, S. L. (2006). Thermal Decomposition of JP-10 Studied by Micro-flowtube Pyrolysis-Mass Spectrometry. *Combust. Flame* 144 (4), 662–674. doi:10.1016/j.combustflame.2005.08.035

Parsinejad, F., Arcari, C., and Metghalchi, H. (2006). Flame Structure and Burning Speed of Jp-10 Air Mixtures. *Combust. Sci. Technol.* 178 (5), 975–1000. doi:10.1080/00102200500270080

Qin, Z., Gong, S., Zhang, X., Bi, Q., Liu, Z., and Liu, G. (2018). Experimental Measurement of JP-10 Density at 267 to 873 K under Pressures up to 6.00 MPa. *J. Chem. Eng. Data* 64 (1), 218–225. doi:10.1021/acs.jced.8b00729

Rocha, R. C. (2021). Structure and Laminar Flame Speed of an Ammonia/Methane/Air Premixed Flame under Varying Pressure and Equivalence Ratio. *Energy fuels.* 35 (9), 7179–7192.

Sakai, Y., Konishi, K., and Ishihara, A. (1996). Tip Opening and Burning Intensity of Bunsen Flames Diluted with Nitrogen. *JSME Int. J. Ser. B, Fluids Therm. Eng.* 39 (1), 164–170. doi:10.1299/jsmeb.39.164

Seiser, R., Niemann, U., and Seshadri, K. (2011). Experimental Study of Combustion of N-Decane and JP-10 in Non-premixed Flows. *Proc. Combust. Inst.* 33 (1), 1045–1052. doi:10.1016/j.proci.2010.06.078

Shang, Y., Shi, J., Ning, H., Zhang, R., Wang, H., and Luo, S. (2019). Ignition Delay Time Measurements and Kinetic Modeling ofCH_4 Initiated by CH_3NO_2. *Fuel* 243, 288–297. doi:10.1016/j.fuel.2019.01.112

Shang, Y., Wang, Z., Ma, L., Shi, J., Ning, H., Ren, W., et al. (2021). Shock Tube Measurement of NO Time-Histories in Nitromethane Pyrolysis Using a Quantum Cascade Laser at 5.26 Mm. *Proc. Combust. Inst.* 38 (1), 1745–1752. doi:10.1016/j.proci.2020.07.026

Shi, J. C., Ye, W., Bie, B. X., Long, X. J., Zhang, R. T., Wu, X. J., et al. (2016). Ignition Delay Time Measurements on $CH_4/CH_3Cl/O_2$/Ar Mixtures for Kinetic Analysis. *Energy fuels.* 30 (10), 8711–8719. doi:10.1021/acs.energyfuels.6b01466

Smith, N. K., and Good, W. D. (1979). Enthalpies of Combustion of Ramjet Fuels. *AIAA J.* 17 (8), 905–907. doi:10.2514/3.61244

Szekely, G. A., and Faeth, G. M. (1983). Effects of Envelope Flames on Drop Gasification Rates in Turbulent Diffusion Flames. *Combust. Flame* 49 (1), 255–259. doi:10.1016/0010-2180(83)90168-2

Tao, Y., Xu, R., Wang, K., Shao, J., Johnson, S. E., Movaghar, A., et al. (2018). A Physics-Based Approach to Modeling Real-Fuel Combustion Chemistry - III. Reaction Kinetic Model of JP10. *Combust. Flame* 198, 466–476. doi:10.1016/j.combustflame.2018.08.022

Vandewiele, N. M., Magoon, G. R., Van Geem, K. M., Reyniers, M.-F., Green, W. H., and Marin, G. B. (2014). Experimental and Modeling Study on the Thermal Decomposition of Jet Propellant-10. *Energy fuels.* 28 (8), 4976–4985. doi:10.1021/ef500936m

Vandewiele, N. M., Magoon, G. R., Van Geem, K. M., Reyniers, M.-F., Green, W. H., and Marin, G. B. (2015). Kinetic Modeling of Jet Propellant-10 Pyrolysis. *Energy fuels.* 29 (1), 413–427. doi:10.1021/ef502274r

Varea, E., Modica, V., Renou, B., and Boukhalfa, A. M. (2013). Pressure Effects on Laminar Burning Velocities and Markstein Lengths for Isooctane-Ethanol-Air Mixtures. *Proc. Combust. Inst.* 34 (1), 735–744. doi:10.1016/j.proci.2012.06.072

Wang, H., Zhang, B., Gong, S., Wang, L., Zhang, X., and Liu, G. (2021). Experimental and Modeling Studies of Exo-Tetrahydrobicyclopentadiene and Tetrahydrotricyclopentadiene Pyrolysis at 1 and 30 Atm. *Combust. Flame* 232, 111536. doi:10.1016/j.combustflame.2021.111536

Wang, S., Gou, H.-j., Fan, B.-c., He, Y.-z., Zhang, S.-t., and Cui, J.-p. (2007). Shock Tube Study of JP-10 Ignition Delay Time. *Chin. J. Chem. Phys.* 20 (1), 48–52. doi:10.1360/cjcp2007.20(1).48.5

Wu, Y., Modica, V., Rossow, B., and Grisch, F. (2016). Effects of Pressure and Preheating Temperature on the Laminar Flame Speed of Methane/air and Acetone/air Mixtures. *Fuel* 185, 577–588. doi:10.1016/j.fuel.2016.07.110

Wu, Y., Rossow, B., Modica, V., Yu, X., Wu, L., and Grisch, F. (2017). Laminar Flame Speed of Lignocellulosic Biomass-Derived Oxygenates and Blends of Gasoline/oxygenates. *Fuel* 202, 572–582. doi:10.1016/j.fuel.2017.04.085

Zettervall, N. (2020). Reduced Chemical Kinetic Reaction Mechanism for JP-10-Air Combustion. *Energy fuels.* 34 (12), 16624–16635. doi:10.1021/acs.energyfuels.0c02971

Zhang, X., Wang, J., Chen, Y., and Li, C. (2021). Effect of CH_4, Pressure, and Initial Temperature on the Laminar Flame Speed of an NH_3-Air Mixture. *ACS Omega* 6 (18), 11857. doi:10.1021/acsomega.1c00080

Zhong, B.-J., Zeng, Z.-M., and Zhang, H.-Z. (2022). An Experimental and Kinetic Modeling Study of JP-10 Combustion. *Fuel* 312, 122900. doi:10.1016/j.fuel.2021.122900

Conflict of Interest: The authors declare that the research was conducted in the absence of any commercial or financial relationships that could be construed as a potential conflict of interest.

Publisher's Note: All claims expressed in this article are solely those of the authors and do not necessarily represent those of their affiliated organizations, or those of the publisher, the editors and the reviewers. Any product that may be evaluated in this article, or claim that may be made by its manufacturer, is not guaranteed or endorsed by the publisher.